SUPPORTING INFORMATION

Single-molecule protein detection in a biofluid using a quantitative nanopore sensor

Avinash Kumar Thakur[1,2] and Liviu Movileanu[1,2,3*]

[1]*Department of Physics, Syracuse University, 201 Physics Building, Syracuse, New York 13244-1130, USA*

[2]*Structural Biology, Biochemistry, and Biophysics Program, Syracuse University,111 College Place, Syracuse, New York 13244-4100, USA*

[3]*Department of Biomedical and Chemical Engineering, Syracuse University, 329 Link Hall, Syracuse, New York 13244, USA*

Keywords: FhuA; Ion channel; Protein-protein Interface; Protein dynamics; Stochastic sensing; Electrophysiology; Membrane Protein Engineering.

*The corresponding author's contact information:
Liviu Movileanu, PhD, Department of Physics, Syracuse University, 201 Physics Building, Syracuse, New York 13244-1130, USA. Phone: 315-443-8078; Fax: 315-443-9103; E-mail: lmovilea@syr.edu

(i) Cloning and mutagenesis of the nanopore sensor and protein analyte. All the genes were developed employing conventional and assembly PCR techniques. They were cloned into the pPR-IBA1 expression vector using respective restriction sites. *obn(ggs)$_2$t-fhua* encoded the peptide adapter (O, MGDRGPEFELGT), fused at the N-terminus of barnase (Bn), a flexible glycine- and serine-rich hexapeptide tether, a truncated outer membrane protein (t-FhuA), and *KpnI* sites at both ends.[1] This gene was created using the *bn* and *t-fhua* genes and assembly PCR reactions. The *bn* gene encoded an H102A mutant, because this lacks RNase activity[2, 3]. Fortuitously, this mutation also converts the non-equilibrium, permanent Bn-Bs interaction into an equilibrium, transient interaction.[3] In this way, OBn(GGS)$_2$FhuA proteins were not toxic to the expression host. The *bs* gene, which encoded the protein analyte, barstar (Bs), featured a double-alanine mutant, C40A/C82A.[4]

(ii) Protein expression and purification. All genes were transformed into *E. coli* BL21(DE3) cells for protein expression. OBn(GGS)$_2$t-FhuA was expressed and purified, as previously reported.[5] For the protein analyte, Bs, transformed cells were grown in Luria-Bertani medium at 37°C until OD_{600} reached a value of ~0.5, after which the temperature was changed to 20°C.[1] After induction in the presence of IPTG, the cells were further cultured for an additional period of ~18 hours at the same temperature. The cells were then centrifugated at 3,700×*g* for 30 min at 4°C, followed by their resuspension in 150 mM KCl, 50 mM Tris-HCl, 5 mM EDTA, pH 8. A Model 110L microfluidizer (Microfluidics, Newton, MA) was used for achieving the cell lysis. To separate the insoluble pellet and supernatant, the lysates were centrifuged at 108,500 × *g* for 30 min at 4°C to separate. The supernatant was further processed for ammonium sulfate precipitation. Then, the supernatant was dialyzed against 20 mM Tris-HCl, pH 8, overnight at 4°C and purified on a Q-Sepharose column (Bio-Rad, Hercules, CA) using a linear salt gradient of 0 - 0.5 M KCl, 20 mM Tris·HCl, pH 8. A refining purification step was conducted by passing pure protein fractions through a Superdex-75 size-exclusion column (SEC; GE Healthcare Life Sciences, Pittsburg, PA).

(iii) Membrane protein refolding. Lyophilized protein samples of OBn(GGS)$_2$t-FhuA were solubilized in 200 mM KCl, 8 M urea, 50 mM Tris-HCl, pH 8 to a final concentration of ~15 µM. Solubilized protein samples were then incubated at room temperature for several hours. n-dodecyl-β-D-maltopyranoside (DDM) was added to denatured samples to a final concertation of 1.5% (w/v). Thereafter, a slow dialysis of protein samples was conducted against the buffer containing 200 mM KCl, 20 mM Tris-HCl, pH 8, at 4 °C for at least 72 h. For single-channel electrical recordings, the protein samples were 20-fold diluted in 200 mM KCl, 20 mM Tris-HCl, pH 8, 0.5% DDM. Protein concentrations were assessed using their molar absorptivity at a wavelength of 280 nm.

(iv) Single-molecule electrophysiology using planar lipid bilayers. Single-channel electrical recordings were conducted using synthetic planar lipid bilayers, as previously published.[6, 7] The protein sample was added to the *cis* side of the chamber (**Fig. 1a**), which was at ground, at a final concentration in a range between 0.3 and 1 ng/µl. The acquisition of single-channel currents was achieved using an Axopatch 200B patch-clamp amplifier (Axon Instruments, Foster City, CA). In all experiments, the electrolyte solution included 300 mM KCl, 10 mM Tris-HCl, pH 8. All single-channel recordings were executed at a temperature of 23 ± 1°C. Statistically significant fit model was determined by using a

standard logarithm likelihood ratio (LLR) test.[8] At a confidence level C = 0.95, the best model was one-exponential fit, unless otherwise stated (see terms resulting from serum constituents). Fetal bovine serum (FBS; Gibco™, catalog number A3160601), was purchased from Fisher Scientific (Pittsburg, PA). FBS was filtered using an 0.2-μm filter, then kept in aliquots at -80°C. In this work, we used a maximum concentration of 5% (v/v) FBS, because the lipid bilayer was stable under these conditions for long recording periods. The total nontarget protein content in FBS was in the range of 30-50 mg/ml (provided by Gibco™). Therefore, the maximum FBS protein concentration for analyzing single-molecule Bs detection was in the range 1.5-2.5 mg/ml. For single-channel electrical recordings, each frozen FBS aliquot was first thawed at 4°C, then incubated at room temperature for at least 30 min. Heat-inactivated fetal bovine serum (HI-FBS) was prepared by incubating the FBS in 56°C water bath for 30 min. The HI-FBS was then allowed to cool down slowly at room temperature for 15 min before being aliquoted and stored at -20°C.[9, 10]

(v) Control single-channel electrical trace of the OBn(GGS)$_2$t-FhuA protein pore at -40 mV.

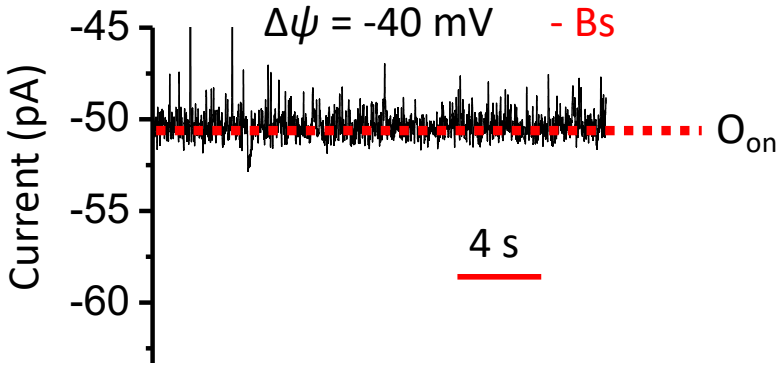

<u>Figure S1:</u> Representative single-channel electrical recording of OBn(GGS)$_2$t-FhuA in the absence of Bs and at an applied transmembrane potential –40 mV. Single-channel electrical trace was further low-pass, 8-pole Bessel filtered at 20 Hz. This single-channel electrical signature was replicated in n = 3 independent experiments. The other experimental conditions were the same as those stated in the main text.

(vi) Standard histograms of the Bs capture and release events at -40 mV.

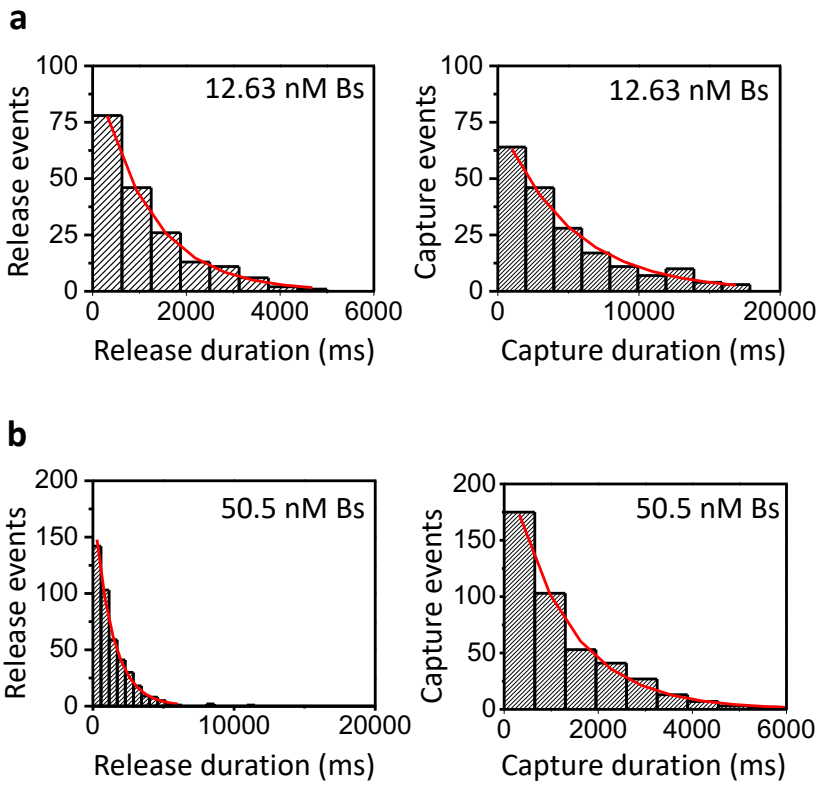

<u>Figure S2:</u> Standard capture and release event histograms in a homogeneous solution.
(**a**) Representative standard histograms of the release (τ_{on}; left) and capture (τ_{off}; right) durations at 12.63 nM Bs. The τ_{on} and τ_{off} values obtained from the fits, in the form of mean ± s.e.m., were 5,053 ± 286 ms (number of events: n = 191) and 1,128 ± 35 ms (n = 184), respectively. (**b**) Representative standard histograms of the release (τ_{on}; left) and capture (τ_{off}; right) durations at 50.5 nM Bs. The τ_{on} and τ_{off} values obtained from the fits, in the form of mean ± s.e.m., were 1,312 ± 50 ms (number of events: n = 420) and 1,236 ± 45 ms (n = 427), respectively. The applied transmembrane potential was –40 mV. The other experimental conditions were stated in the caption of **Fig. 1b**.

(vii) FBS constituents produced long-lived current blockades at a high negative potential.

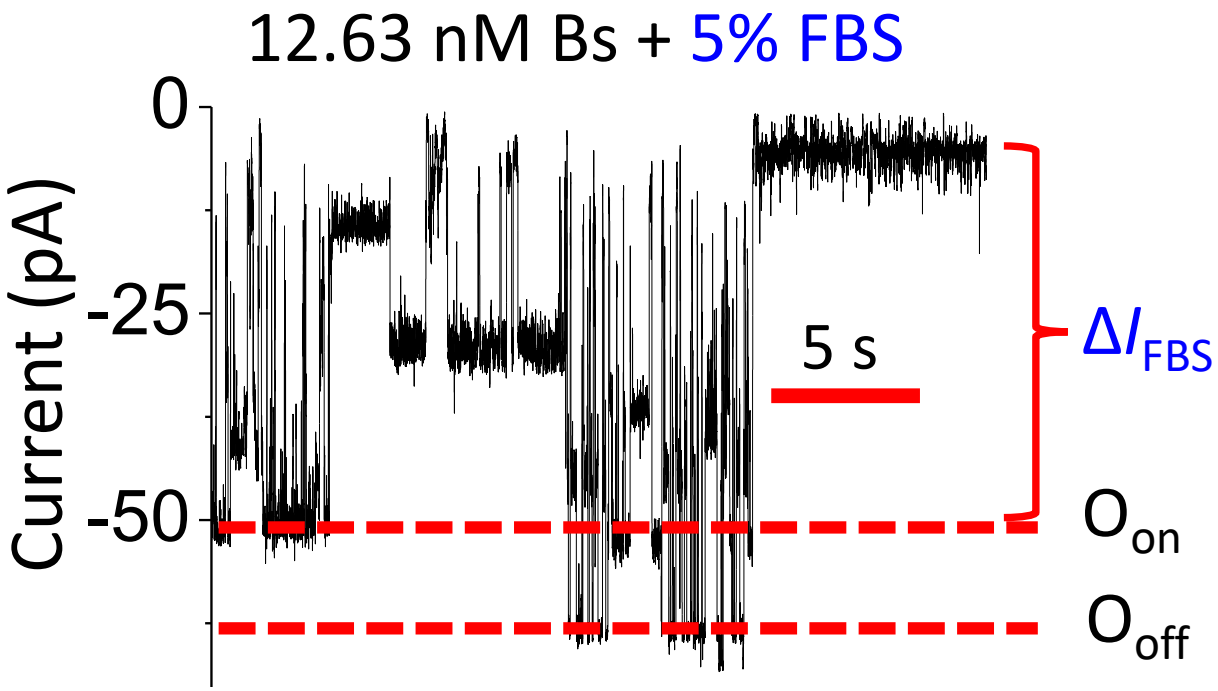

<u>Figure S3:</u> Fetal bovine serum (FBS) causes very long-lived current blockades at an applied tansmembrane potential of –40 mV. This figure illustrates a representative single-channel electrical measurement of OBn(GGS)$_2$t-FhuA when 50.5 nM Bs was added to the *cis* side. The transmembrane potential was –40 mV. The buffer solution in cis side also contained 5% (v/v) FBS. This single-channel electrical signature was replicated in two independent experiments. All recordings were performed in 300 mM KCl, 10 mM Tris·HCl pH 8, and at a temperature of 23 ± 1°C.

(viii) Voltage dependence of the differential current.

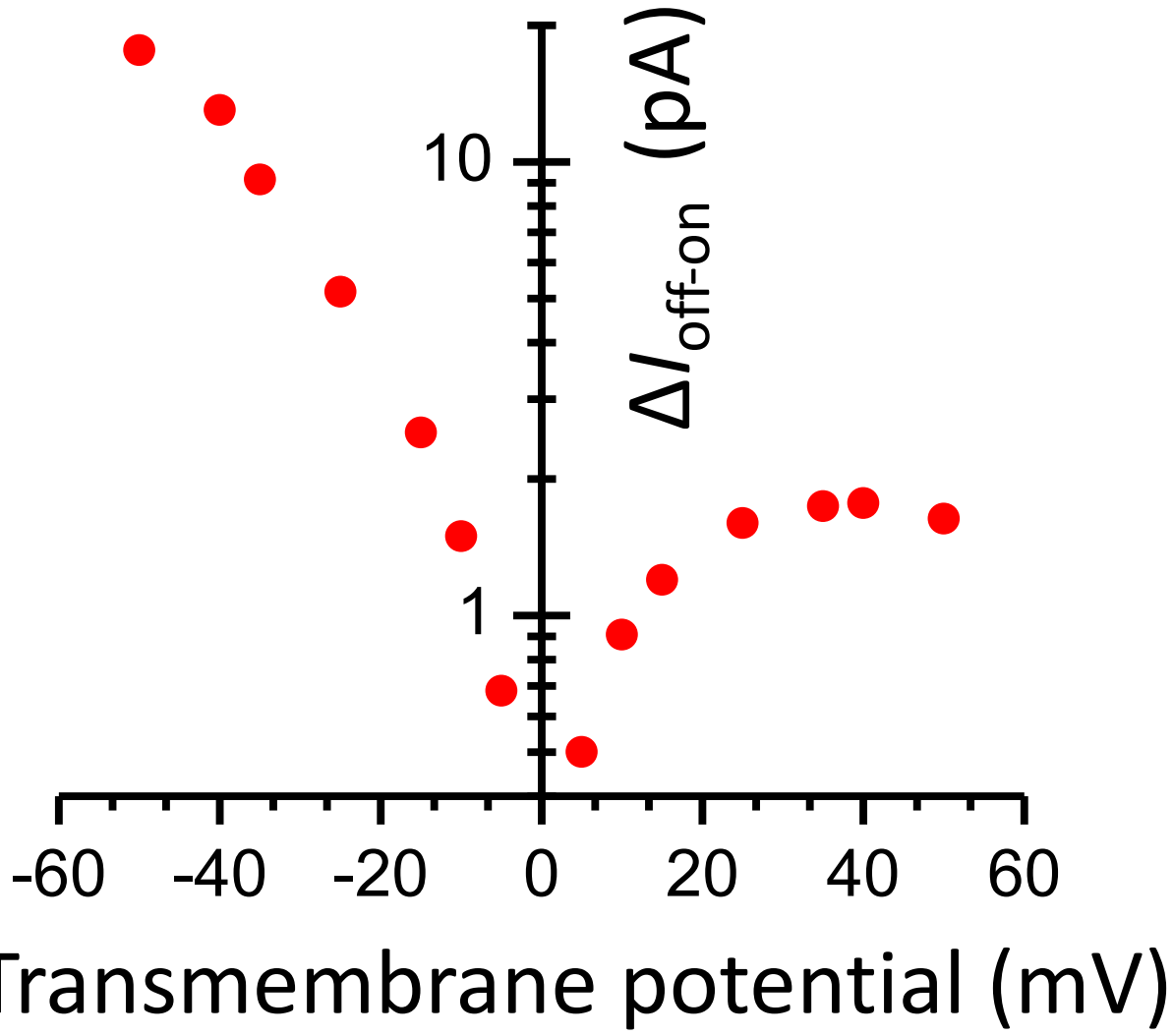

Figure S4: **The current-voltage scatter plot of the differential current, ΔI_{off-on}.** This data was recorded using OBn(GGS)$_2$t-FhuA in the presence of 100.9 nM Bs. ΔI_{off-on} is the absolute current difference between the Bs-free (O_{on}) and Bs-bound (O_{off}) open substates. The other experimental conditions were the same as those stated in the main text in **Fig. 1b**. This plot resulted from data acquisition of a single experiment.

(ix) The SNR of the O_{on} and O_{off} substates is improved at an applied transmembrane potential of +15 mV.

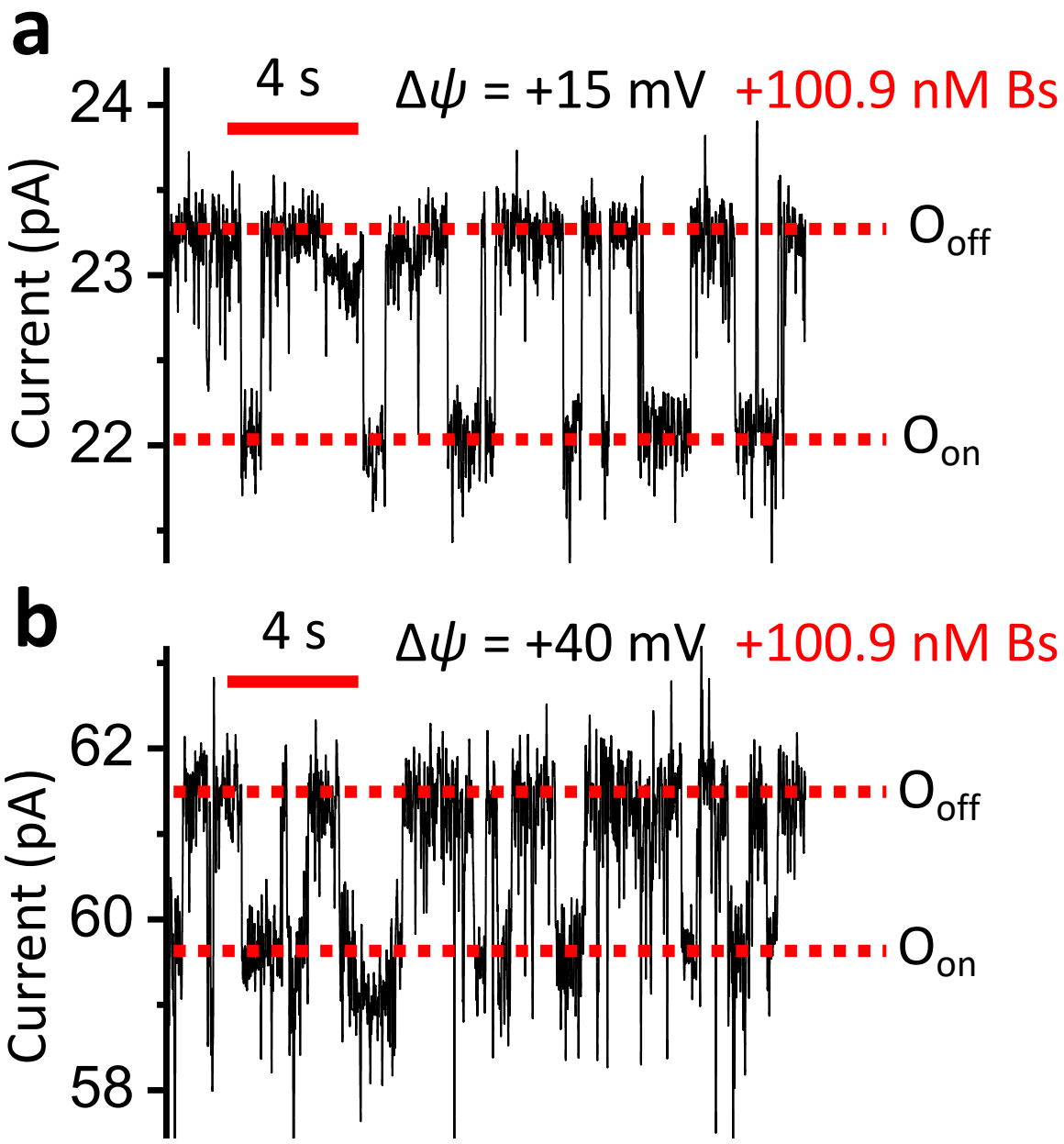

Figure S5: **Qualitative comparison of signal-to-noise of single-channel electrical recordings of OBn(GGS)$_2$t-FhuA in the presence of 100.9 nM Bs and at applied transmembrane potentials of +15 mV (a) and +40 mV (b)**. Both single-channel electrical traces were further low-pass, 8-pole Bessel filtered at 20 Hz. Single-channel electrical signatures shown in **(a)** and **(b)** were replicated in n = 3 independent experiments. The other experimental conditions were the same as those stated in the main text in **Fig. 1b**.

(x) Control single-channel electrical trace of the OBn(GGS)$_2$t-FhuA protein pore at +15 mV.

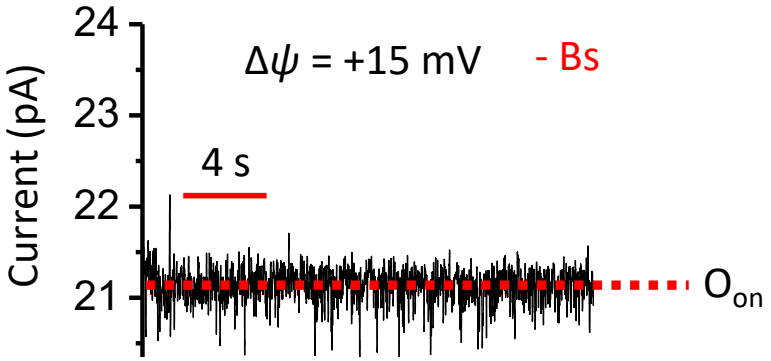

Figure S6: Representative single-channel electrical recording of OBn(GGS)$_2$t-FhuA in the absence of Bs and at an applied transmembrane potential of +15 mV. Single-channel electrical trace was further low-pass, 8-pole Bessel filtered at 20 Hz. This single-channel electrical signature was replicated in n = 3 independent experiments. The other experimental conditions were the same as those stated in the main text in **Fig. 1b**.

(xi) Standard histograms of the Bs capture and release events at +15 mV.

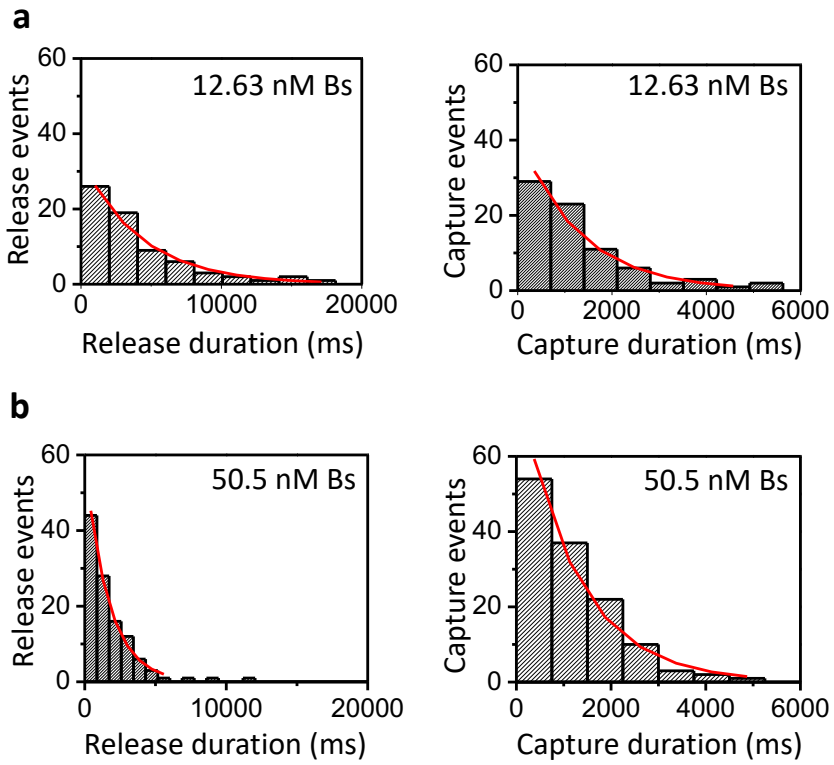

Figure S7: Representative release and capture event histograms. (**a**) Representative standard histograms of the release (τ_{on}; left) and capture (τ_{off}; right) durations of the Bs reversible captures at 12.63 nM Bs. The τ_{on} and τ_{off} values obtained from the fits, in the form of mean ± s.e.m., were 4,244 ± 316 ms (number of events: n = 70) and 1,292 ± 163 ms (n = 77), respectively. (**b**) Representative

standard histograms of the release (τ_{on}; left) and capture (τ_{off}; right) durations at 50.5 nM Bs. The τ_{on} and τ_{off} values obtained from the fits, in the form of mean ± s.e.m., were 1,657 ± 81 ms (number of events: n =129) and 1,214 ± 136 ms (n = 130), respectively. The applied transmembrane potential was +15 mV. The other experimental conditions were stated in the caption of **Fig. 1c**.

(xii) Analyses of the kinetic rate constants in homogeneous (FBS-free) and heterogeneous (FBS) solutions.

Table S1. The release (τ_{on}) and capture (τ_{off}) durations, as well as the association (k_{on}) and dissociation (k_{off}) rate constants determined at various protein analyte concentrations ([Bs]). The applied transmembrane potential was +15 mV. These data points were used to construct panels of **Fig. 1h**. They represent mean ± s.d. over a number of n distinct experiments. n is listed on the first column of the table (*left side*). The other experimental conditions were the same as those indicated in the caption of **Fig. 1**.

n	[Bs]	τ_{on} (ms)	τ_{off} (ms)	$k_{on} \times 10^{-7}$ ($M^{-1}s^{-1}$)	k_{off} (s^{-1})
5	12.63	4339 ± 764	1075 ± 249	1.87 ± 0.3	0.98 ± 0.27
3	25.25	2398 ± 1141	1070 ± 105	2.00 ± 1.1	0.94 ± 0.09
3	50.5	1608 ± 268	1049 ± 173	1.26 ± 0.22	0.97 ± 0.16
4	100.01	671 ± 260	1122 ± 156	1.64 ± 0.59	0.91 ± 0.13

Table S2. Table illustrating the association and dissociation rate constants determined in the absence (-) and presence (+) of 5% (v/v) FBS. The applied transmembrane potential was +15 mV. The equilibrium dissociation constant, K_d, was k_{off}/k_{on}. Values show mean ± s.e.m. from the curve fit of **Fig. 1h**. The other experimental conditions were the same as those stated in the main text in **Fig. 1**.

FBS	$k_{on} \times 10^{-7}$ ($M^{-1}s^{-1}$)	k_{off} (s^{-1})	K_d (nM)
-	1.59 ± 0.08	0.95 ± 0.02	60 ± 4
+	1.67 ± 0.09	0.86 ± 0.03	52 ± 3

(xiii) Other pieces of supporting information.

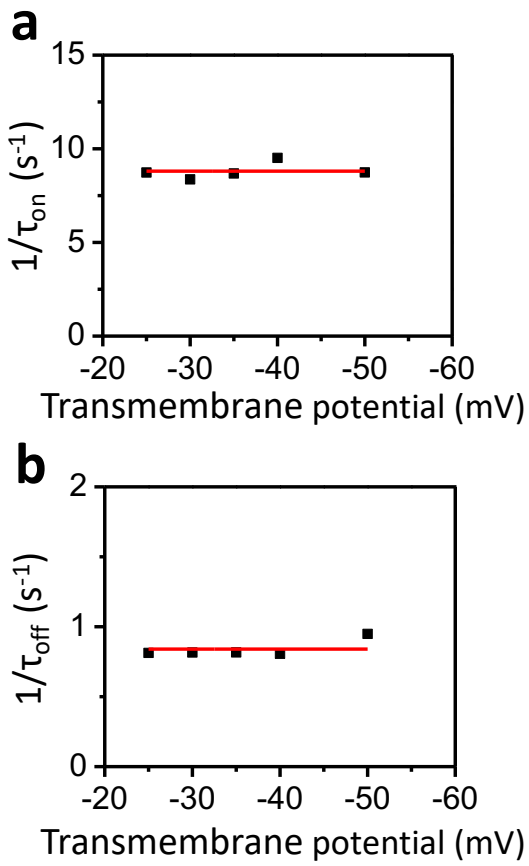

Figure S8: **Voltage dependence of the Bn-Bs interactions using OBn(GGS)$_2$t-FhuA.** Plots show the reciprocals of the association **(a)** and dissociation **(b)** rates constants. The flatness of both plots indicate that the recorded Bn-Bs interactions were voltage independent. These single-channel electrical recordings were conducted at a concertation of 627.2 nM Bs. The other experimental conditions were the same as those stated in the caption of **Fig. 1b**. This plot resulted from data acquisition of a single experiment.

Table S3. The release (τ_{on}) and capture (τ_{off}) durations, as well as the association (k_{on}) and dissociation (k_{off}) rate constants determined at various protein analyte concentrations ([Bs]) and in the presence of 5% (v/v) FBS. The applied transmembrane potential was +15 mV. These data points were used to construct panels of **Fig. 2e**. They represent mean ± s.d. over a number of n distinct experiments. n is listed on the first column of the table (*left side*). The other experimental conditions were the same as those indicated in the caption of **Fig. 2**.

n	[Bs]	τ_{on} (ms)	τ_{off} (ms)	*Kon* 10^{-7} ($M^{-1}s^{-1}$)*	*Koff (s-1)*
3	12.63	4283 ± 311	1170 ± 81	1.86 ± 0.14	0.86 ± 0.06
3	25.25	2888 ± 439	1242 ± 55	1.39 ± 0.19	0.81 ± 0.04
3	50.5	1573 ± 469	1214 ± 22	1.33 ± 0.38	0.82 ± 0.02
3	100.01	577 ± 118	1051 ± 111	1.76 ± 0.32	0.96 ± 0.09

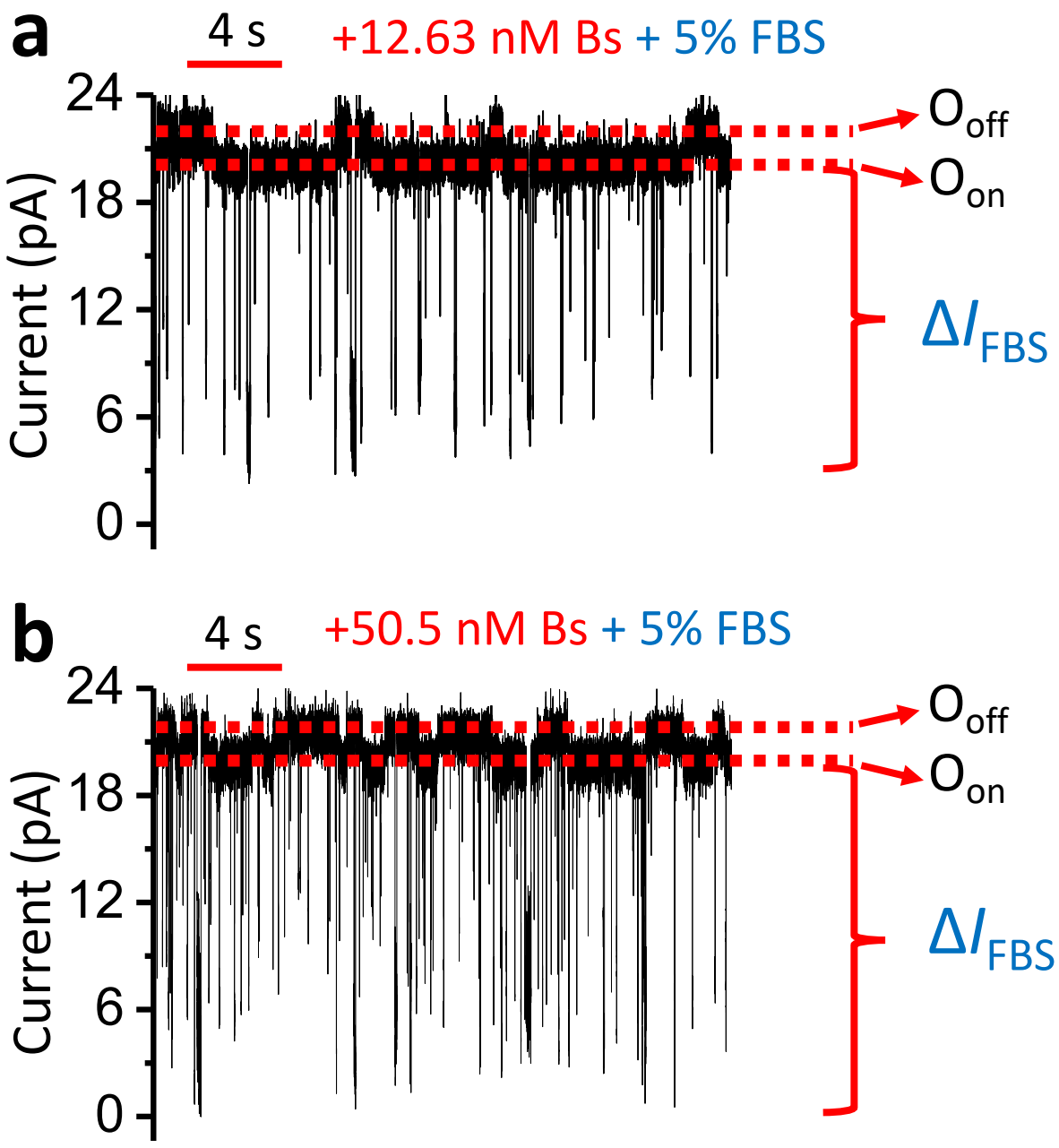

Figure S9: **Representative single-channel electrical recordings of OBn(GGS)$_2$t-FhuA in the presence of 5% (v/v) FBS, as well as 12.63 nM Bs (a) and 50.5 nM Bs (b).** The transmembrane potential was +15 mV. Both single-channel electrical traces were further low-pass 8-pole Bessel filtered at 500 Hz. Single-channel electrical signatures shown in **(a)** and **(b)** were replicated in n = 3 independent experiments. The other experimental conditions were the same as those stated in the caption of **Fig. 1b**.

Table S4. Fitting results for Figure 2f at 12.63 nM Bs added to the *cis* side. The *cis* side of the chamber also contained 5% (v/v) FBS.

Type	P	τ_{off} (ms)
1	0.502 ± 0.090	1.53 ± 0.18
2	0.343 ± 0.130	7.79 ± 0.55
3	0.134 ± 0.140	30.4 ± 1.2
4	0.021 ± 0.063	199 ± 4

Values are mean ± s.e.m. The other experimental conditions were the same as those stated in the caption of **Fig. 2b**.

Table S5. Fitting results for Figure 2f at 50.5 nM Bs added to the *cis* side. The *cis* side of the chamber also contained 5% (v/v) FBS.

Type	P	τ_{off} (ms)
1	0.525 ± 0.084	1.62 ± 0.16
2	0.309 ± 0.082	7.91 ± 0.46
3	0.146 ± 0.085	37.9 ± 0.7
4	0.021 ± 0.040	355 ± 27

Values are mean ± s.e.m. The other experimental conditions were the same as those stated in the caption of **Fig. 2b**.

The dwell times of the four FBS-induced events at 5% (v/v) FBS were the following (mean ± s.e.m.; n=3): $\tau_{off\text{-}1}$ = 1.4 ± 0.1 ms, $\tau_{off\text{-}2}$ = 7.4 ± 0.2 ms, $\tau_{off\text{-}3}$ = 34.7 ± 2.2 ms, and $\tau_{off\text{-}4}$ = 282 ± 30 ms with their corresponding probabilities P_1 = 0.51 ± 0.03, P_2 = 0.31 ± 0.01, P_3 = 0.14 ± 0.01, and P_4 = 0.02 ± 0.01, respectively (**Fig. 2g**; **Supporting Information**, **Tables S6-S9**).

Table S6. Event probability, inter-event duration, dwell time, and event frequency of FBS-induced current blockades in the presence of 12.63 nM Bs. These experiments were conducted using 5% (v/v) FBS.

Event type	P	τ_{on} (ms)	τ_{off} (ms)	f (s^{-1})
1	0.472 ± 0.034	221 ± 83	1.37 ± 0.21	2.138 ± 0.633
2	0.324 ± 0.059		7.50 ± 0.50	1.436 ± 0.370
3	0.156 ± 0.020		33.7 ± 5.2	0.692 ± 0.126
4	0.048 ± 0.040		235 ± 54	0.214 ± 0.190

P indicates the event probability. f shows the event frequency. Values are mean ± s.d. (n=3). The other experimental conditions were the same as those stated in the caption of **Fig. 2b**.

Table S7. Event probability, inter-event duration, dwell time, and event frequency of FBS-induced current blockades in the presence 25.25 nM Bs. These experiments were conducted using 5% (v/v) FBS.

Type	P	τ_{off} (ms)	τ_{on} (ms)	f (s^{-1})
1	0.493 ± 0.067	1.04 ± 0.22	414 ± 134	0.941 ± 0.331
2	0.317 ± 0.029	6.28 ± 2.59		0.603 ± 0.172
3	0.143 ± 0.033	32.2 ± 11.0		0.287 ± 0.140
4	0.048 ± 0.025	319 ± 161		0.095 ± 0.058

P indicates the event probability. *f* shows the event frequency. Values are mean ± s.d. (n=3). The other experimental conditions were the same as those stated in the caption of **Fig. 2b**.

Table S8. Event probability, inter-event duration, dwell time, and event frequency of FBS-induced current blockades in the presence of 50.48 nM Bs. These experiments were conducted using 5% (v/v) FBS.

Type	P	τ_{off} (ms)	τ_{on} (ms)	f (s^{-1})
1	0.567 ± 0.038	1.25 ± 0.41	362 ± 296	2.220 ± 2.243
2	0.241 ± 0.093	7.08 ± 0.87		1.193 ± 1.423
3	0.124 ± 0.028	36.2 ± 14.1		0.555 ± 0.668
4	0.068 ± 0.057	354 ± 117		0.143 ± 0.038

P indicates the event probability. *f* shows the event frequency. Values are mean ± s.d. (n=3). The other experimental conditions were the same as those stated in the caption of **Fig. 2b**.

Table S9. Event probability, inter-event duration, dwell time, and event frequency of FBS-induced current blockades in the presence of 100.91 nM Bs. These experiments were conducted using 5% (v/v) FBS.

Type	P	τ_{off} (ms)	τ_{on} (ms)	f (s^{-1})
1	0.551 ± 0.083	1.59 ± 0.25	161 ± 44	2.816 ± 0.626
2	0.319 ± 0.040	7.72 ± 0.89		1.705 ± 0.674
3	0.116 ± 0.045	44.6 ± 13.7		0.623 ± 0.311
4	0.013 ± 0.004	373 ± 125		0.073 ± 0.043

P indicates the event probability. *f* shows the event frequency. Values are mean ± s.d. (n=3). The other experimental conditions were the same as those stated in the caption of **Fig. 2b**.

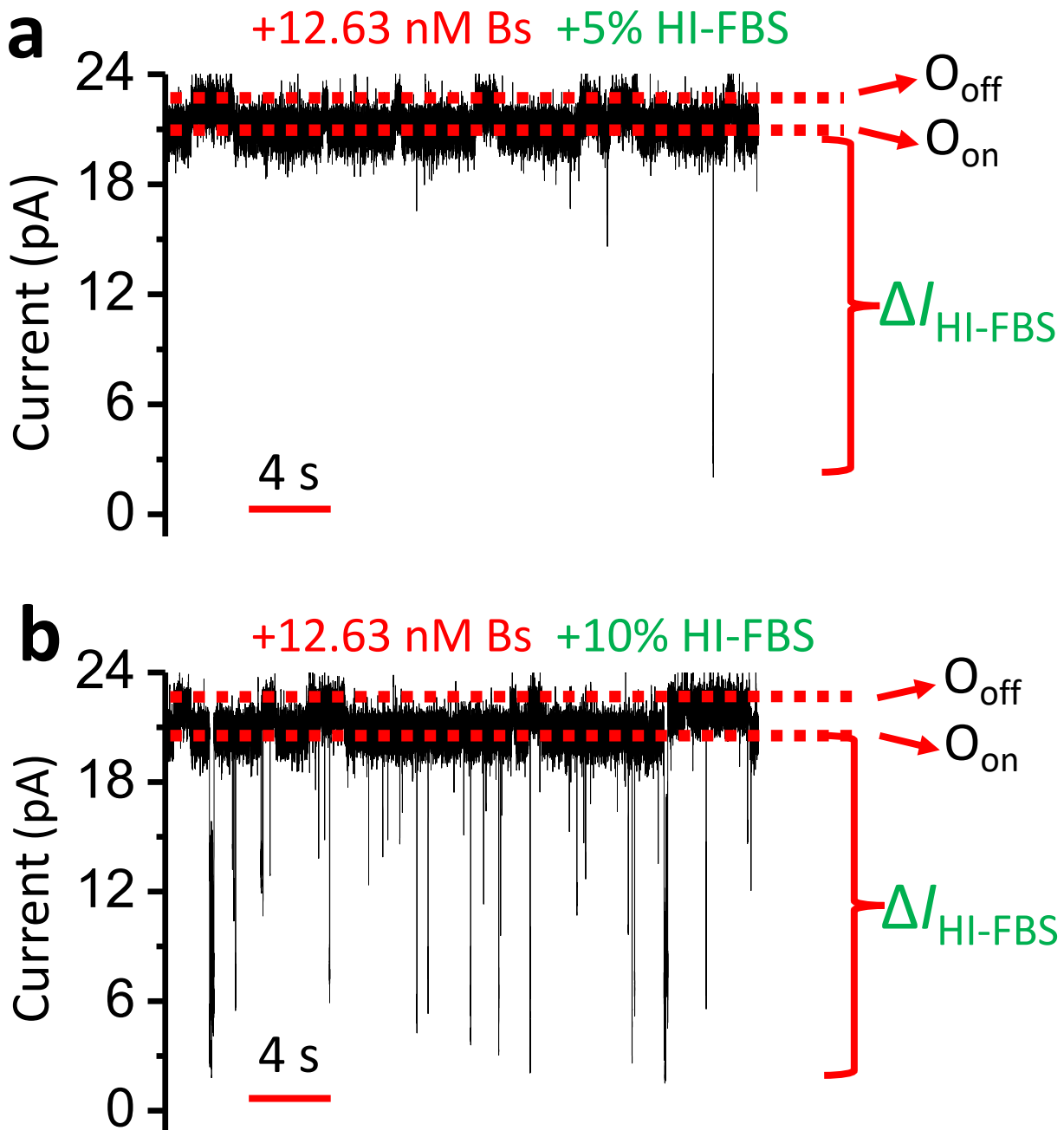

Figure S10: Representative single-channel electrical recordings of OBn(GGS)$_2$t-FhuA in the presence of 12.63 nM Bs, as well as 5% (v/v) HI-FBS (a) and 10% (v/v) HI-FBS (b). The applied transmembrane potential was +15 mV. Both single-channel electrical traces were further low-pass 8-pole Bessel filtered at 500 Hz. Single-channel electrical signatures shown in **(a)** and **(b)** were replicated in n = 3 independent experiments. The other experimental conditions were the same as those stated in the caption of **Fig. 2b**.

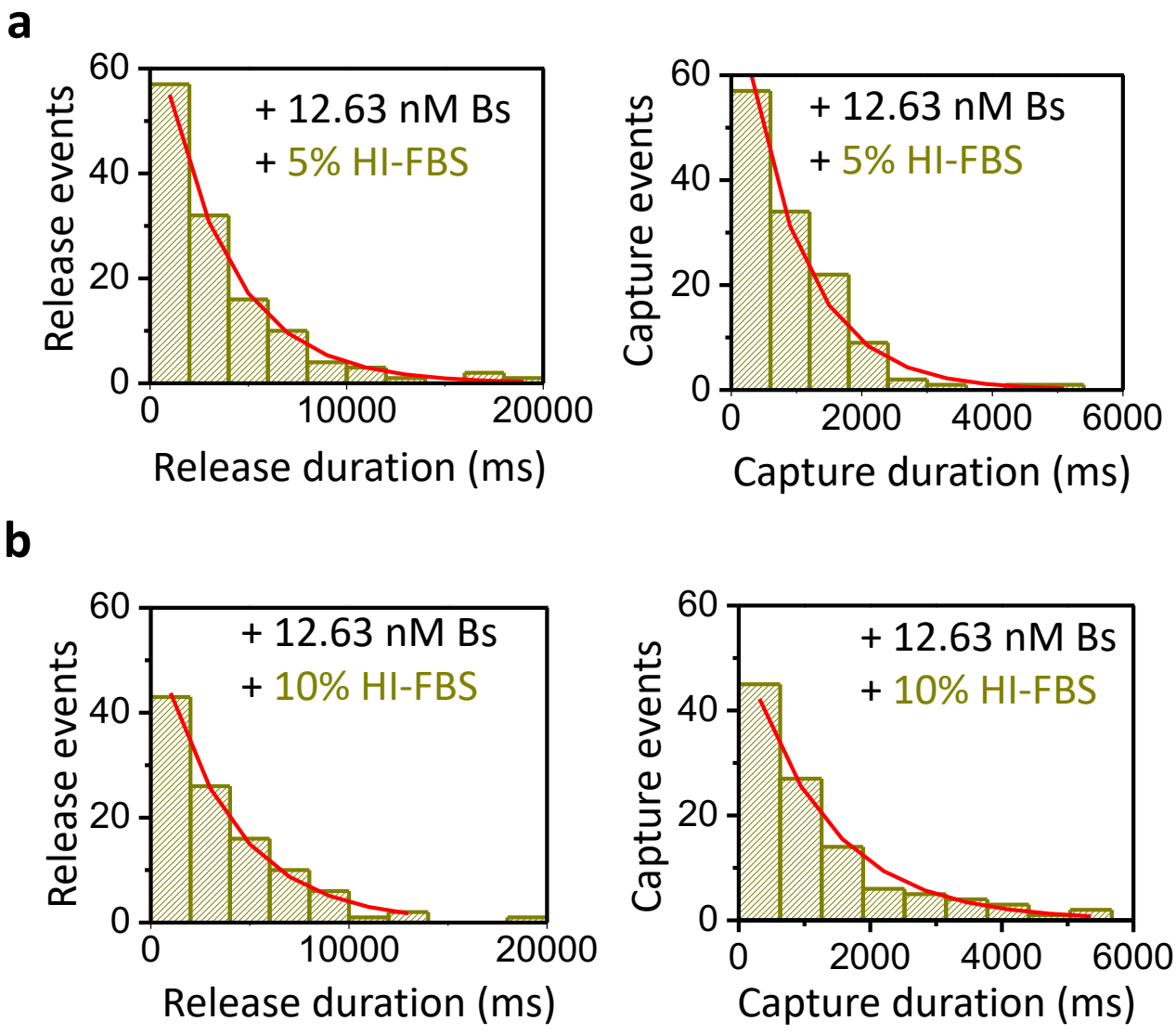

Figure S11: Standard capture and release event histograms in HI-FBS. (**a**) Representative standard histograms of the release (τ_{on}; left) and capture durations (τ_{off}; right) in 5% (v/v) HI-FBS and at a concentration of 12.63 nM Bs. The τ_{on} and τ_{off} values obtained from the fits, in the form of mean ± s.e.m., were 3,434 ± 132 ms (number of events: n = 126) and 909 ± 78 ms (n = 128), respectively. (**b**) Representative standard histograms of the release (τ_{on}; left) and capture duration (τ_{off}; right) of the reversible Bs captures recorded in 10% (v/v) HI-FBS and at a concentration of 12.63 nM Bs. The τ_{on} and τ_{off} values obtained from the fits, in the form of mean ± s.e.m., were 3,719 ± 174 ms (number of events: n = 106) and 1,257 ± 91 ms (n = 107), respectively.

Table S10. The release (τ_{on}) and capture (τ_{off}) durations, as well as the association (k_{on}) and dissociation (k_{off}) rate constants determined at 12.63 nM Bs and in the presence of 5% (v/v) HI-FBS, 10% (v/v) HI-FBS, or 20% (v/v) HI-FBS. The applied transmembrane potential was +15 mV. These data points were used to construct panels of **Fig. 3d**. They represent mean ± s.d. over a number of n distinct experiments. n is listed on the first column of the table (*left side*). The other experimental conditions were the same as those indicated in the caption of **Fig. 3**.

n	HI-FBS (%) (v/v)	τ_{on} (ms)	τ_{off} (ms)	$k_{on} \times 10^{-7}$ ($M^{-1}s^{-1}$)	k_{off} (s^{-1})
3	5	3990 ± 539	1022 ± 343	2.01 ± 0.28	1.05 ± 0.32
3	10	4180 ± 428	1195 ± 252	1.91 ± 0.20	0.84 ± 0.18
3	20	4881 ± 519	1071 ± 108	1.63 ± 0.17	0.93 ± 0.09

Table S11. Event probability, inter-event duration, dwell time, and event frequency of HI-FBS-induced current blockades in the presence of 12.63 nM Bs. These experiments were conducted using 5% (v/v) HI-FBS.

Type	P	τ_{off} (ms)	τ_{on} (ms)	f (s^{-1})
1	0.842 ± 0.083	0.42 ± 0.12	7940 ± 2231	0.114 ± 0.030
3	0.159 ± 0.083	15.4 ± 6.5		0.024 ± 0.020

Values are mean ± s.d. (n=3). The other experimental conditions were the same as those stated in the caption of **Fig. 3**.

Table S12. Event probability, inter-event duration, dwell time, and event frequency of HI-FBS-induced current blockades in the presence of 12.63 nM Bs. These experiments were conducted using 10% (v/v) HI-FBS.

Type	P	τ_{off} (ms)	τ_{on} (ms)	f (s^{-1})
1	0.601 ± 0.077	1.15 ± 0.08	576 ± 167	0.823 ± 0.129
2	0.246 ± 0.076	7.5 ± 4.1		0.3602 ± 0.208
3	0.111 ± 0.026	41.7 ± 25		0.161 ± 0.074
4	0.042 ± 0.015	428 ± 347		0.056 ± 0.018

Values are mean ± s.d. (n=3). The other experimental conditions were the same as those stated in the caption of **Fig. 3**.

Table S13. Event probability, inter-event duration, dwell time, and event frequency of HI-FBS-induced current blockades in the presence of 12.63 nM Bs. These experiments were conducted using 20% (v/v) HI-FBS.

Type	P	τ_{off} (ms)	τ_{on} (ms)	f (s^{-1})
1	0.670 ± 0.083	1.45 ± 0.42	358 ± 41	1.428 ± 0.353
2	0.217 ± 0.063	7.50 ± 5.12		0.448 ± 0.088
3	0.081 ± 0.019	50.5 ± 30.0		0.170 ± 0.036
4	0.033 ± 0.024	444 ± 330		0.067 ± 0.043

Values are mean ± s.d. (n=3). The other experimental conditions were the same as those stated in the caption of **Fig. 3**.

SUPPORTING REFERENCES

1. Thakur, A. K.; Movileanu, L., Real-Time Measurement of Protein-Protein Interactions at Single-Molecule Resolution using a Biological Nanopore. *Nat. Biotechnol.* **2019,** *37* (1), 96-101.

2. Schreiber, G.; Fersht, A. R., Interaction of barnase with its polypeptide inhibitor barstar studied by protein engineering. *Biochemistry* **1993,** *32* (19), 5145-5150.

3. Schreiber, G.; Fersht, A. R., Energetics of protein-protein interactions: analysis of the barnase-barstar interface by single mutations and double mutant cycles. *J. Mol. Biol* **1995,** *248* (2), 478-486.

4. Guillet, V.; Lapthorn, A.; Hartley, R. W.; Mauguen, Y., Recognition between a bacterial ribonuclease, barnase, and its natural inhibitor, barstar. *Structure* **1993,** *1* (3), 165-76.

5. Thakur, A. K.; Larimi, M. G.; Gooden, K.; Movileanu, L., Aberrantly Large Single-Channel Conductance of Polyhistidine Arm-Containing Protein Nanopores. *Biochemistry* **2017,** *56* (36), 4895-4905.

6. Mohammad, M. M.; Howard, K. R.; Movileanu, L., Redesign of a plugged beta-barrel membrane protein. *J. Biol. Chem.* **2011,** *286* (10), 8000-8013.

7. Larimi, M. G.; Mayse, L. A.; Movileanu, L., Interactions of a Polypeptide with a Protein Nanopore Under Crowding Conditions. *ACS nano* **2019,** *13* (4), 4469-4477.

8. Couoh-Cardel, S.; Hsueh, Y. C.; Wilkens, S.; Movileanu, L., Yeast V-ATPase Proteolipid Ring Acts as a Large-conductance Transmembrane Protein Pore. *Sci. Rep.* **2016,** *6*, 24774.

9. Simon, J.; Muller, J.; Ghazaryan, A.; Morsbach, S.; Mailander, V.; Landfester, K., Protein denaturation caused by heat inactivation detrimentally affects biomolecular corona formation and cellular uptake. *Nanoscale* **2018,** *10* (45), 21096-21105.

10. Soltis, R. D.; Hasz, D.; Morris, M. J.; Wilson, I. D., The effect of heat inactivation of serum on aggregation of immunoglobulins. *Immunology* **1979,** *36* (1), 37-45.